LUND UNIVERSITY

Numerical investigations of the laminating effect in laminated beams

Serrano, Erik; Larsen, Hans Jörgen

Published in:
Journal of Structural Engineering

DOI:
10.1061/(ASCE)0733-9445(1999)125:7(740)

1999

Link to publication

Citation for published version (APA):
Serrano, E., & Larsen, H. J. (1999). Numerical investigations of the laminating effect in laminated beams. *Journal of Structural Engineering*, *125*(7), 740-745. https://doi.org/10.1061/(ASCE)0733-9445(1999)125:7(740)

Total number of authors:
2

Creative Commons License:
CC BY-NC-ND

General rights
Unless other specific re-use rights are stated the following general rights apply:
Copyright and moral rights for the publications made accessible in the public portal are retained by the authors and/or other copyright owners and it is a condition of accessing publications that users recognise and abide by the legal requirements associated with these rights.
• Users may download and print one copy of any publication from the public portal for the purpose of private study or research.
• You may not further distribute the material or use it for any profit-making activity or commercial gain
• You may freely distribute the URL identifying the publication in the public portal

Read more about Creative commons licenses: https://creativecommons.org/licenses/

Take down policy
If you believe that this document breaches copyright please contact us providing details, and we will remove access to the work immediately and investigate your claim.

LUND UNIVERSITY

PO Box 117
221 00 Lund
+46 46-222 00 00

LUND UNIVERSITY | LUND INSTITUTE OF TECHNOLOGY
Division of Structural Mechanics | Sweden 1997 | Report TVSM–3023

NUMERICAL INVESTIGATIONS OF THE LAMINATING EFFECT IN LAMINATED BEAMS

Submitted for publication in ASCE – Journal of Structural Engineering

ERIK SERRANO AND HANS JØRGEN LARSEN

LUND UNIVERSITY | LUND INSTITUTE OF TECHNOLOGY
Division of Structural Mechanics | Sweden 1997 | Report TVSM–3023
CODEN: LUTVDG/(TVSM–3023)/1–16/(1997) | ISSN 0281–6679

NUMERICAL INVESTIGATIONS OF THE LAMINATING EFFECT IN LAMINATED BEAMS

Submitted for publication in ASCE – Journal of Structural Engineering

ERIK SERRANO AND HANS JØRGEN LARSEN

Numerical Investigations of The Laminating Effect in Laminated Beams

Erik Serrano[1] and Hans Jørgen Larsen[2]

Abstract: The paper presents numerical results concerning the so-called laminating effect of laminated beams. Using the finite element method it is shown that the stress redistribution often asssumed to take place around weak zones is not necessarily true. A fracture mechanics approach to a possible explanation for the laminating effect is also presented. Here a nonlinear fracture mechanics model is used to verify a hand calculation formula based on linear elastic fracture mechanics. An important outcome is that for an initially cracked laminated beam, the failure mode tends to be dominated by shear failure in the outermost lamination, as the lamination thickness decreases.
Keywords: laminated beams, stress distribution, fracture mechanics, laminating effect

INTRODUCTION

In order to predict the behaviour of glued-laminated timber (glulam), it is essential to understand the effect of strength increase of laminations as a result of bonding them into a glulam beam, the so-called laminating effect. This effect, is often expressed as a laminating factor, k_{lam}, given by:

$$k_{lam} = \frac{f_{m,beam}}{f_{t,lam}} \tag{1}$$

where $f_{t,lam}$ is the tensile strength of the lamination and $f_{m,beam}$ is the bending strength of the beam, evaluated using ordinary beam theory.
The laminating effect has been explained by Foschi and Barrett (1980) and Larsen (1982) as an effect of the following:

1. In a glulam beam the defects are smeared out resulting in a more homogeneous material than solid wood. The probability of a defect's having a

[1]Division of Structural Mechanics, Lund University, P.O Box 118, SE-221 00, Lund, Sweden. Telephone: +46 46 222 81 62. Fax: +46 46 222 44 20.
[2]Division of Structural Mechanics, Lund University, P.O Box 118, SE-221 00, Lund, Sweden. Telephone: +46 46 222 73 70. Fax: +46 46 222 44 20.

serious influence on the strength of the beam is less than it is in a single lamination.

2. A single lamination tested in pure tension, will bend due to knots and other anomalies. This is due to the stiffness not being constant over the cross-section of the lamination. If the same lamination was contained in a glulam beam, the rest of the beam would prevent such bending.

3. If a lamination that is tested contains knots or other zones of low stiffness, a pure tensile test does not represent the true stress distribution found in a beam that is subjected to pure bending. The adjacent stiffer and stronger laminations would then take up a larger part of the tensile stresses.

The above three explanations are related to the beam being built up of laminations. In addition to this, $k_{lam} \neq 1.0$ can be due to a nonlinear stress-strain performance of the material or due to different strength in compression than in tension. These causes for $k_{lam} \neq 1.0$ are however not related to the number and thickness of the laminations.
An effort to explain and quantify the different contributions to the laminating effect has been presented by Falk and Colling (1995). Experimental data showing such laminating factors are found in the works of Larsen (1982), and Falk et al. (1994). Larsen found that for different beam compositions the laminating factor varied from 1.06 to 1.68. The investigation of Falk et al. yielded laminating factors in the range of 1.35 to 1.65.
In the present study emphasis is put on the third item above, and on the possibility of introducing new explanations to the laminating effect based on fracture mechanics. The study presented here is a part of a research project dealing with the mechanical behaviour of finger-joints and laminated beams presented in Serrano (1997).

PRESENT STUDIES

Two types of simulations of laminated beam behaviour are presented here. The first is a linear elastic analysis of a beam subjected to a pure bending moment, using varying stiffness parameters. These analyses were carried out in order to study the influence of stiffness variation on the stress distribution in a beam. The second type of laminated beam simulations concerns the nonlinear behaviour of the bond line of the outermost lamination. These simulations were performed in order to study the possibility of predicting the laminating effect by use of a fracture mechanical approach.

INFLUENCE OF STIFFNESS VARIATION ON STRESS DISTRIBUTION

Background

In analysing a beam of non-homogeneous cross-section, an assumption commonly made is that plane sections perpendicular to the beam axis remain plane and perpendicular when the beam is deformed. This assumption leads to the well-known result of a piecewise linear stress distribution over the cross-section of a glulam beam consisting of laminations differing in their modulus of elasticity. According to these assumptions, a zone of lower stiffness would be subjected to stresses of lesser magnitude, in line with the reduction in stiffness. It is often claimed that such a "weak" zone (e.g. a knot or a finger-joint) of lower stiffness, and probably thus of lower strength too than adjacent material, would be subjected to stresses of smaller magnitude and would therefore not have so strong effect on global beam strength. The present analyses shows that a low stiffness zone is not necessarily relaxed in the way described above.

Analyses

The load-case analysed is that of a glulam beam subjected to pure bending. The linear elastic analyses are performed using plane stress, 4-node, finite elements. At the boundaries where the bending moments are applied, plane sections of the beam are assumed to remain plane during loading. The beam is 315 mm in height, (7 laminations, each 45 mm thick) 600 mm in length and 100 mm in width. There is assumed to be a zone of lower stiffness in the outer tension lamination. The weak zone is 45 mm in height, its length varying from 7.5 mm to 600 mm in the different analyses. The finite element mesh used in the analyses is shown in Figure 1. In the weak zone, all the stiffness parameters are reduced by the same percentage, the surrounding material being assigned the engineering constants of E_x=12000 MPa, E_y=400 MPa, G_{xy}=600 MPa, and ν_{xy}=0.53.
Two types of analyses were performed. In the first series of analyses, the length of the weak zone was varied from the same length as the beam (600 mm) to the length of two finite elements in the fine-meshed area (7.5 mm), see Figure 1. In these cases, the stiffness parameters E_x, E_y and G_{xy} in the weak zone were assumed to be reduced by 25%. In the second series of analyses, the influence of varying the stiffness reduction was investigated. The weak zone, 30 mm in length, was reduced in stiffness by 25, 50, 75 and 100%, respectively. In both types of analyses, the height of the weak zone was taken to be the same as the lamination thickness, i.e. 45 mm.

Results

The results of the finite element analyses are shown in Figures 2–5. The stress distributions shown in these figures all correspond to the same bending moment.

The normalized stress shown is the stress divided by the maximum stress as calculated by the conventional flexure formula for a homogeneous beam. Figure 2 shows the influence of the length of the weak zone on the stress distribution in the mid-section. As expected, when the weak zone is as long as the beam, the stress distribution is indeed piecewise linear, in accordance with beam theory. A reduction in the extension of the weak zone results in a redistribution of the axial stresses. In the limiting case, as the length of the weak zone approaches zero, the stress distribution is found to approach the linear one expected in a homogeneous cross-section. According to beam theory, the length of the weak zone should not affect the stress distribution at all. Figure 3 shows the stress distribution in the mid-section of the beam for a length of the weak zone of 30 mm. In this figure is also shown the stress distribution as predicted by beam theory. The reduction of the stresses in the weak zone is very local. In Figure 4 the influence on the axial tensile *force* (i.e. the mean stress in the outermost lamination) in the weak zone is shown. In the case of a weak zone 30 mm in length, the axial force is reduced by only about 3% for a stiffness reduction of 25%. According to beam theory the reduction would be 15.3%, which coincides with the FE-result obtained when the weak zone is extended all along the beam.

In Figure 5 the influence of the stiffness reduction on the stress distribution in the mid-section is shown. The four curves represent a 25, 50, 75 and 100% reduction in stiffness, respectively. As expected, for a 100% reduction in stiffness, the stresses in the weak zone are zero, since the weak zone then represents a hole or a notch. The analyses suggest that the simple assumption that a local and proportional reduction in stiffness and strength has only minor influence on beam strength is *not* valid for small zones such as knots and finger-joints. Since the stress reduction in a small zone is far from proportional to the stiffness reduction, the stress is closer to the strength of the material in a small weak zone than one would expect by intuition.

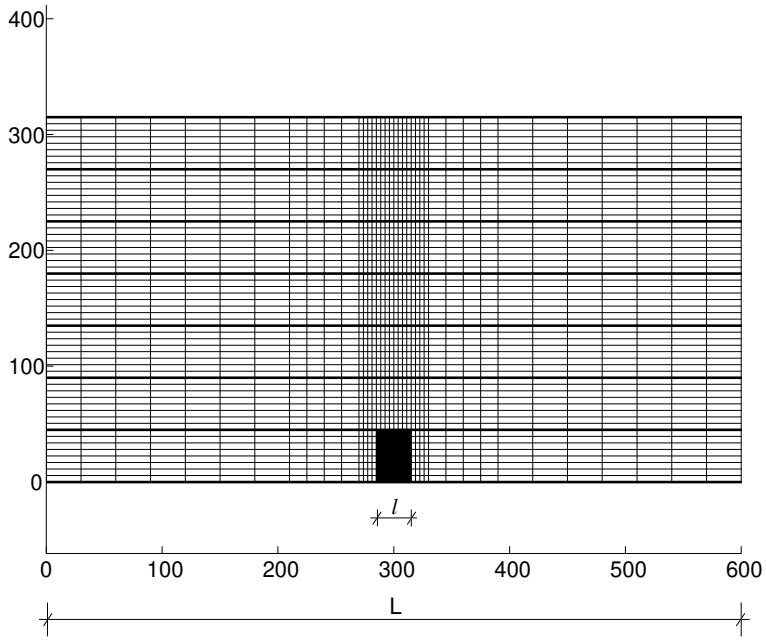

Figure 1: Finite element mesh. The dark area is the weak zone, having in the figure a length of 30 mm.

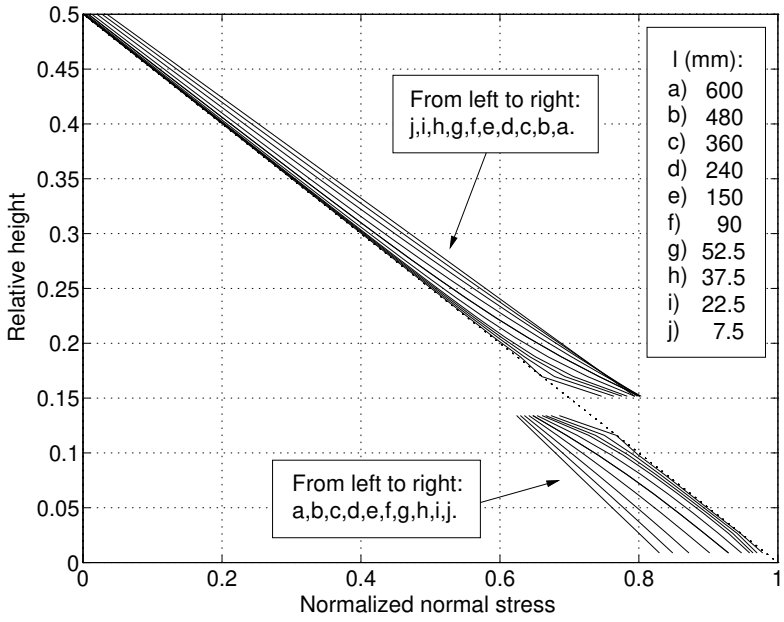

Figure 2: Influence of the length of the weak zone on the stress distribution in the mid-section in the case of a stiffness reduction of 25% in the weak zone.

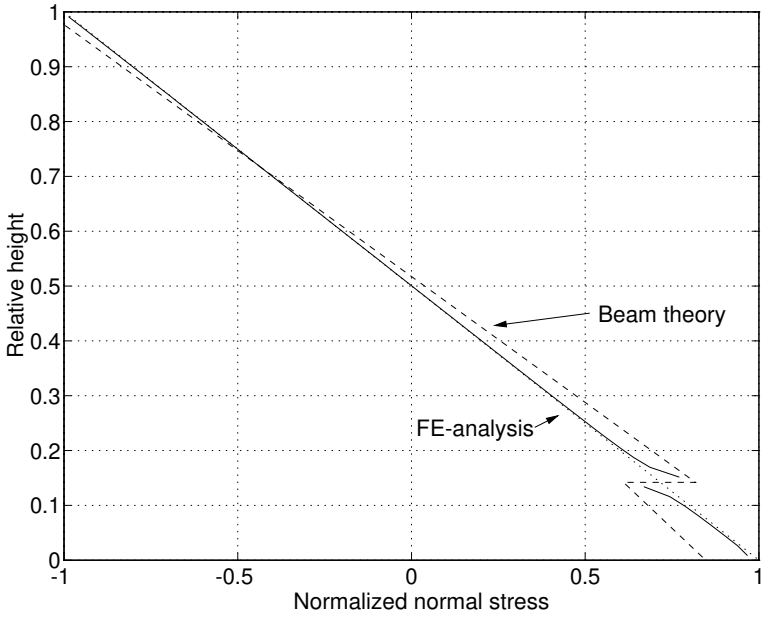

Figure 3: Stress distribution in the mid-section of the beam for a length of the weak zone of 30 mm as calculated with plane stress finite elemnts (solid line) and according to beam theory (dashed line). The stiffness reduction is 25%.

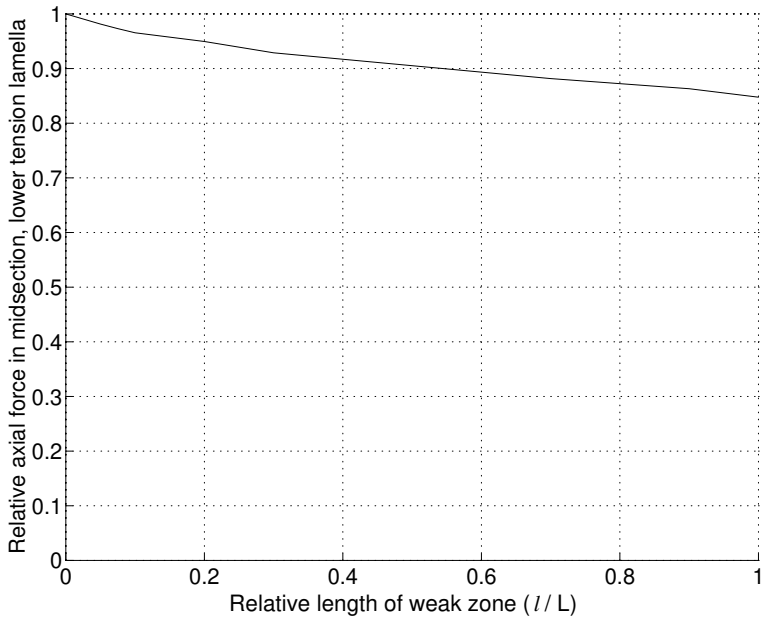

Figure 4: Influence of the length of the weak zone on the axial tensile force in the outermost lamination. The stiffness reduction is 25%.

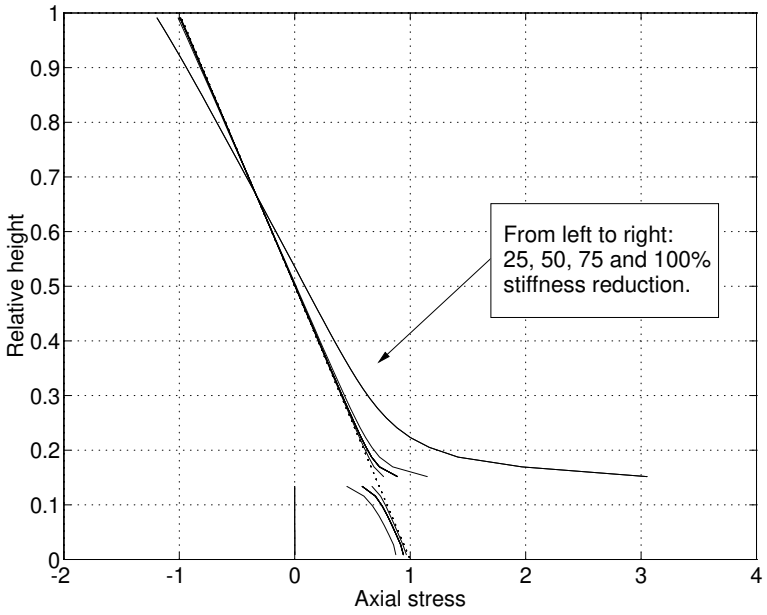

Figure 5: Influence of the magnitude of stiffness reduction on the stress distribution in the mid-section. The curves represent 25, 50, 75 and 100% stiffness reduction, respectively. The weak zone has a length of 30 mm.

LAMINATING EFFECT AS PREDICTED BY FRACTURE MECHANICS

General Remarks

Consider a glulam beam consisting of several layers of laminations, each having the same thickness Δh, Figure 6. The load case studied is that of a beam subjected to a pure bending moment. In the outer tension lamination, the beam contains a weak zone representing e.g. a knot or a finger-joint. When the weak zone has failed, the load-bearing capacity of the beam and its subsequent behaviour, may be governed by crack propagation in the direction of the beam. The grain direction is assumed to coincide with the length axis of the beam. This situation is illustrated in Figure 6

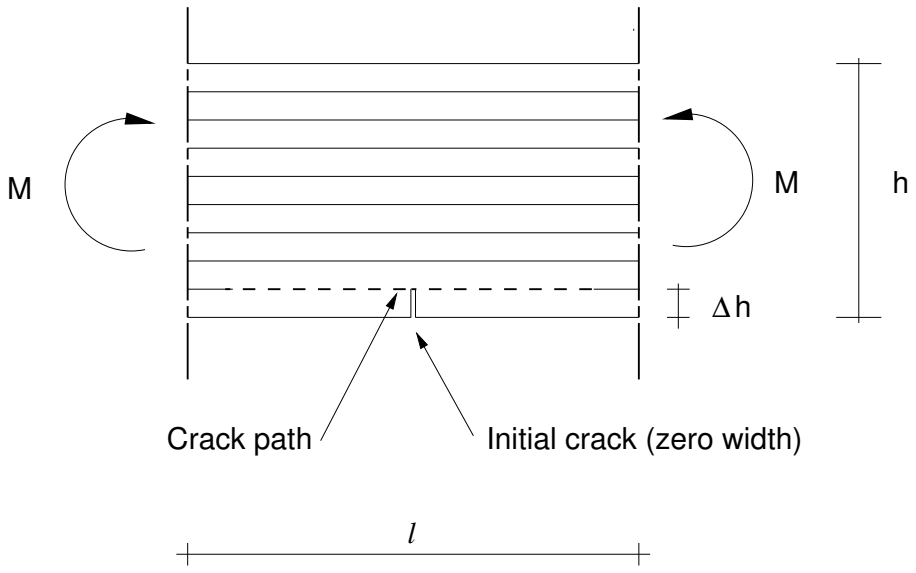

Figure 6: A laminated beam with an initial crack of a length equal to the lamination thickness. The dashed line represents the crack path at crack propagation.

A Hand Calculation Formula

Based on the assumptions of *linear elastic* fracture mechanics (LEFM), Petersson (1994) derived an expression for the critical bending moment, M_c, at which a crack will propagate:

$$M_c = \sqrt{\frac{2 \cdot G_c \cdot b \cdot E_x \cdot I}{1/\alpha^3 - 1}} \tag{2}$$

where E_x denotes the modulus of elasticity in the fibre direction, G_c the fracture energy at crack propagation (the energy required to extend the crack a unit area), I the moment of inertia of the beam ($bh^3/12$, b is the beam width and h its height) and α the ratio $(h - \Delta h)/h$. To use Equation (2), the fracture energy

must be known. Since the fracture energy for wood varies from approximately 200–400 J/m^2 for pure mode I to about three times this value for pure mode II, the current mixed mode state must be known for an accurate choice of the value of G_c to be made. However, if the mode I value of G_c is used with (2) what is obtained is a lower bound and often a fairly accurate approximation.
If a more sophisticated analysis is desired, one needs not only to calculate the current degree of mixed mode at crack propagation, but also to take account of the effect of the gradual development of the fracture zone and its non-zero size. A nonlinear fracture mechanics approach such as that used in the present work allows this to be solved. To verify Equation (2), a series of finite element analyses were performed using a bond line model based on nonlinear fracture mechanics described in Wernersson (1994). In this model gradual fracture softening and mixed mode are considered.

A Finite Element Analysis

The case studied is that of a beam of height $h = 450$ mm and length $l = 1600$ mm, cf. Figure 6, subjected to a pure bending moment, assuming the plane end-sections to remain plane during deformation. To investigate the laminating effect, five different lamination thicknesses Δh were studied, namely 50, 25, 12.5, 6.25 and 3.125 mm. In each case the length of the initial crack was assumed to be equal to the lamination thickness, as indicated in Figure 6. The elements representing the bond line and located along the crack path are 0.8 mm long. The bondline data needed to define its behaviour includes the strengths in pure mode I and II and the corresponding fracture energies. The values of these quantities were chosen in accordance with those reported by Wernersson (1994) i.e. 6.5 and 10 MPa strength in modes I and II, respectively, the corresponding fracture energies being 360 and 980 J/m^2.
The wood was modelled as being a linear elastic orthotropic material with the engineering constants of E_x=16800 MPa, E_y=560 MPa, G_{xy}=1050 MPa, and ν_{xy}=0.45. The elements representing the wood are 4-node isoparametric plane stress elements or triangular constant strain elements for mesh refining. The deformed beam at maximum load is shown in Figure 7.
The results of the five different lamination thickness simulations are shown in Figure 8. The five simulations are represented by circles, whereas the dashed lines represent results based on Equation (2) with $G_c = G_{Ic} = 360$ J/m^2 and $G_c = G_{IIc} = 980$ J/m^2. A major outcome of the simulations is that, as the lamination thickness decreases, the crack propagation is increasingly governed by mode II.
Another way of presenting the results of the finite element analyses is shown in Figure 9, displaying the strongly nonlinear behaviour of the beam. This figure presents the formal bending stress in the outer lamination as a function of the position of the tip of the fracture process zone (as measured from the symmetry line). For all the analyses, the load reached a plateau-value. Since this corresponds

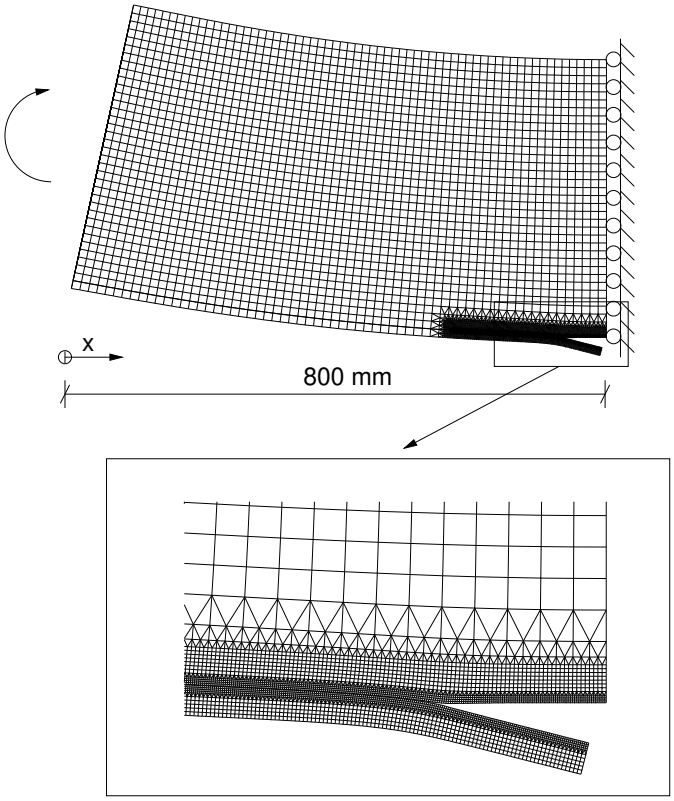

Figure 7: The deformed beam at maximum load. The crack has extended 50–60 mm. The displacements are magnified by a factor of 30.

to the propagation of a fully developed fracture process zone, constant in shape, LEFM can be expected to provide an accurate estimate of the peak load, provided the proper mixed-mode value of G_c is employed.

Figure 10 shows the stress distribution along the bond line of the outermost lamination at peak load for the cases of Δh being 12.5 and 3.125 mm, respectively. The 3.125 mm lamination gives a stress distribution that differs considerably from the distributions obtained for the thicker laminations. The thicker laminations have stress distributions very similar to that obtained for the case of Δh being 12.5 mm. The main difference is the size of the fracture process zone, which for the 3.125 mm lamination is approximately 48 mm long. For all the thicker laminations, the fracture process zone is approximately 25 mm long.

It turns out that the mixed mode state varies during crack propagation. The

current mixed mode state is defined by:

$$\varphi = \arctan\left(\frac{\delta_s}{\delta_n}\right) \tag{3}$$

where δ_s and δ_n are the relative displacements between two points on either side of the bondline. Indices s and n denote shear and normal deformation respectively. A failure in pure opening mode (mode I) corresponds to $\delta_s = 0 \Rightarrow \varphi = 0°$ and a pure shear crack propagation corresponds to $\delta_n = 0 \Rightarrow \varphi = 90°$. The curves of Figure 11 are given in terms of the mixed mode angle φ, as defined by (3) versus the crack tip position. The value of φ is calculated at the peak shear stress position.

Finally, Figure 12 shows how the different contributions of mode I and mode II fracture depend on the lamination thickness. Again, it can be seen that a thin lamination yields almost pure mode II fracture.

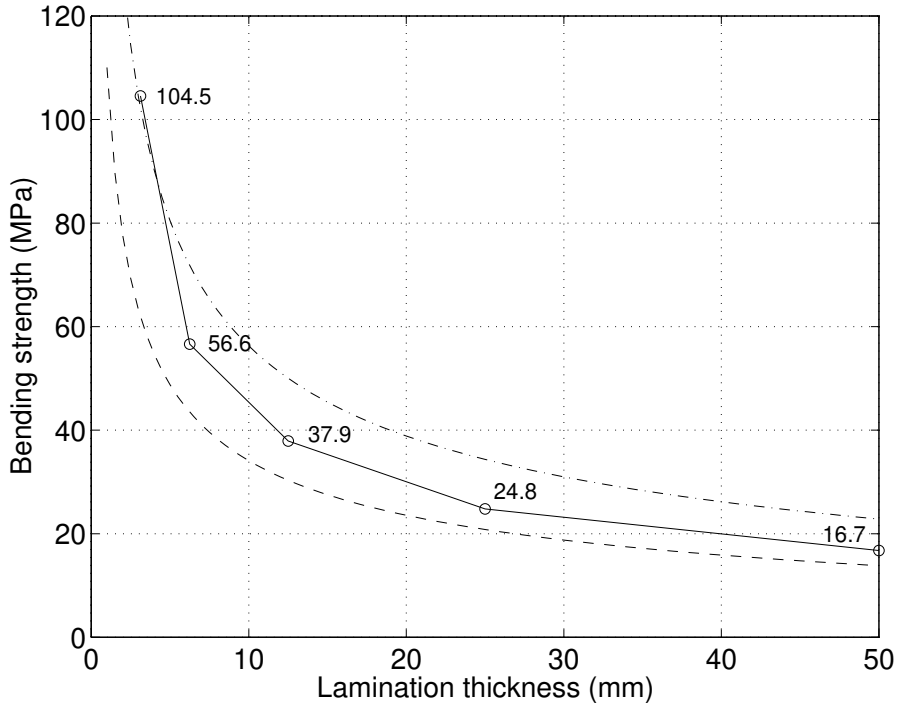

Figure 8: Formal bending strength, $6M/(\,bh^2)$, versus lamination thickness for a laminated beam 450 mm in height. The circles represent results of FE-simulations. The dashed lines represent results based on Equation (2) for $G_c = G_{Ic}$ (dashed) and $G_c = G_{IIc}$ (dashed-dotted).

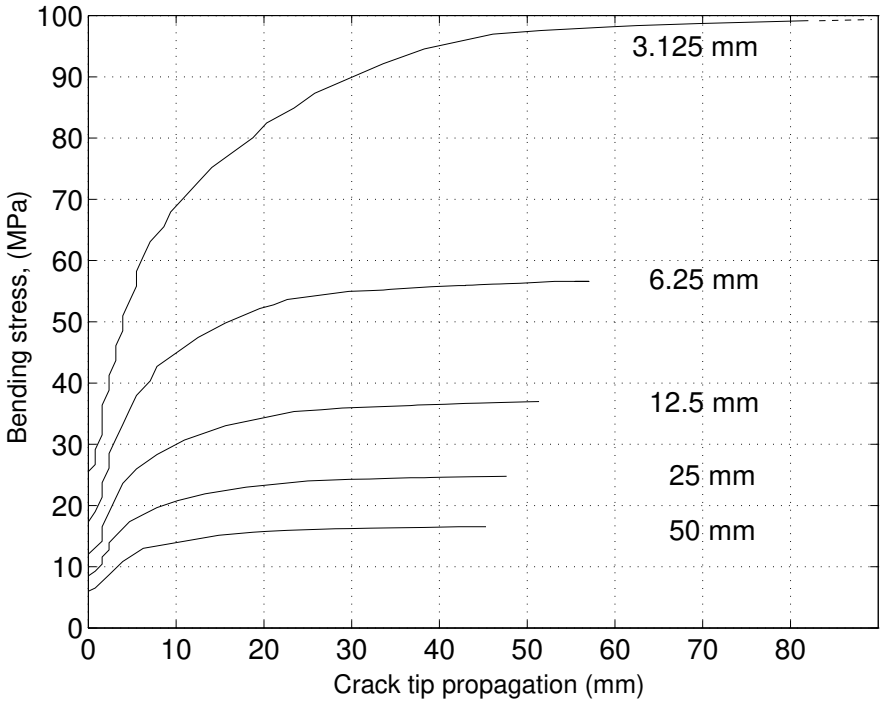

Figure 9: Formal bending stress, $6M/(\,bh^2)$, versus crack tip position for various lamination thicknesses.

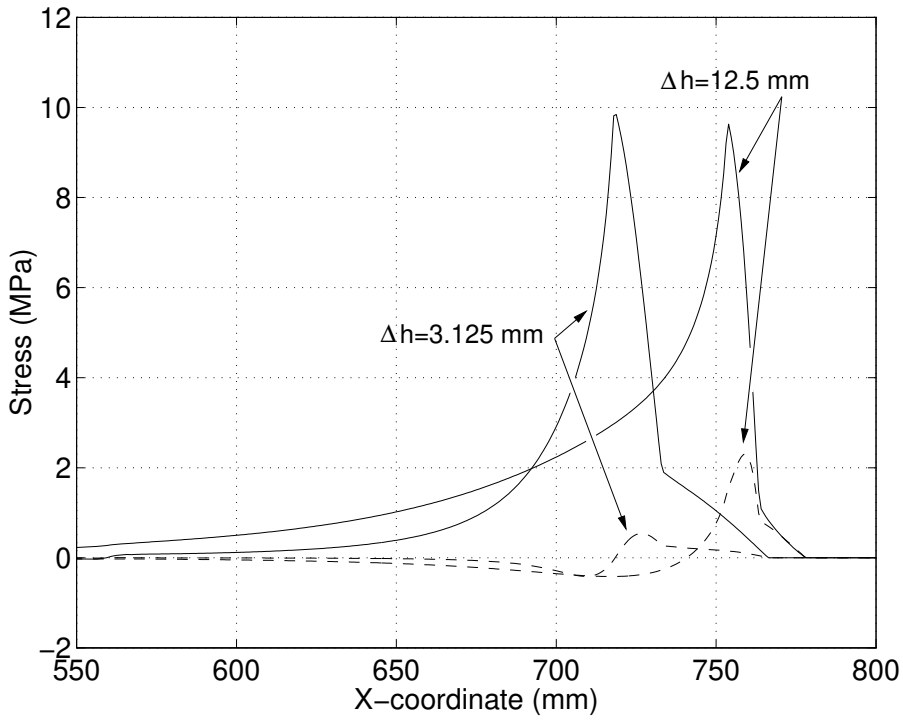

Figure 10: Stress distribution along the bond line of the outermost lamination at peak load. The solid lines correspond to shear stress and the dashed to normal stress.

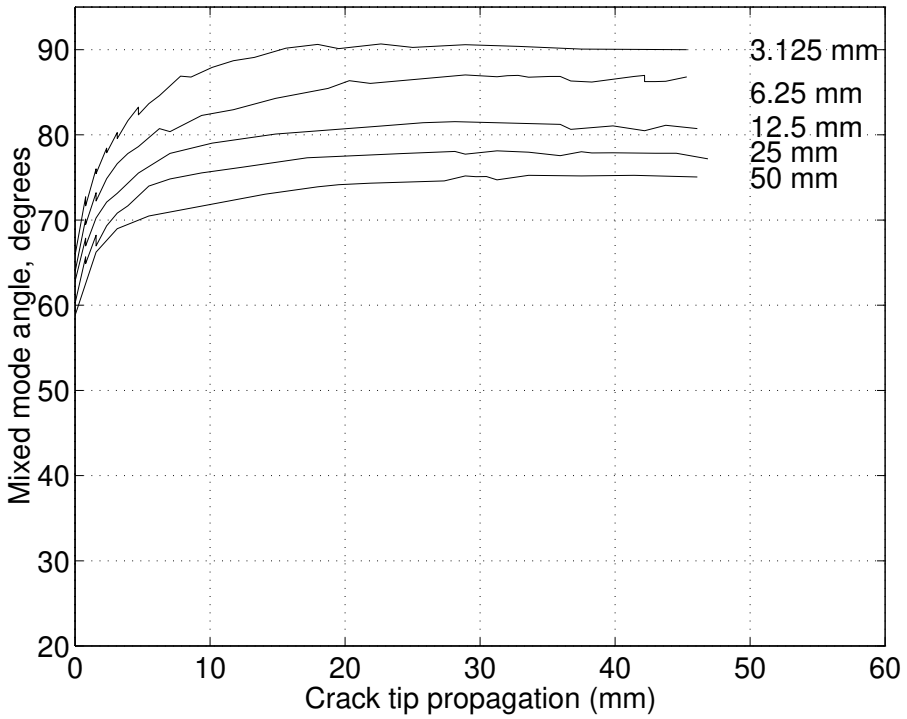

Figure 11: Mixed mode angle φ as defined in Equation (3) versus crack tip position for different lamination thicknesses.

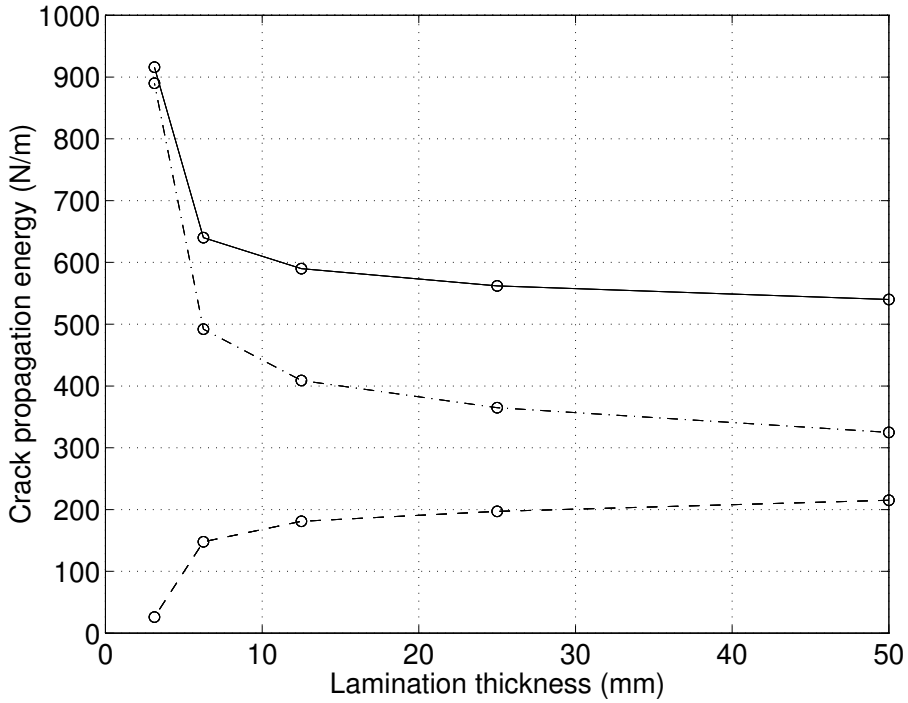

Figure 12: Energy consumption for different lamination thicknesses at the propagation of a fully developed fracture zone (solid line). The dashed lines represent the contributions of mode I (dashed) and mode II (dashed-dotted), respectively.

CONCLUSIONS

The following conclusions can be drawn from the work presented in this paper:

- For a laminated beam with a weak zone of small dimensions in comparison to the dimensions of the beam, the stress redistribution around this weak zone is negligible.
- For initially cracked laminated beams in bending the failure mode along the outermost lamination tends to be more dominated by shear failure as the lamination thicknesses decrease.

APPENDIX I. REFERENCES

Falk, R. H., and Colling, F. (1995). "Laminating effects in glued-laminated timber beams" *J. Struct. Engrg.*, ASCE, 121(12), 1857–1863.

Falk, R. H., Solli, K. H. and Aasheim, E. (1992) "The performance of glued laminated beams manufactured from machine stress graded norwegian spruce." *Rep. no. 77.* Norsk Treteknisk Institutt, Oslo, Norway.

Foschi, R. O., and Barrett, J. D. (1980). "Glued-Laminated Beam Strength: A Model." *J. Sruct. Div.*, ASCE, 106(8), 1735–1754.

Larsen, H. J. (1982). "Strength of glued laminated beams. Part 5." *Report no. 8201.* Intituttet for Bygningsteknik. Aalborg, Denmark.

Petersson, H. (1994). "Fracture design criteria for wood in tension and shear." *Proc. Pacific Timber Engrg. Conf.*, Gold Coast Australia.

Serrano, E. (1997). "Finger-joints for Laminated Beams. Experimental and numerical studies of mechanical behaviour." *Report TVSM-3021*, Lund University, Division of Structural Mechanics, Lund, Sweden.

Wernersson, H. (1994). "Fracture characterization of wood adhesive joints." *Report TVSM-1006*, Lund University, Division of Structural Mechanics, Lund, Sweden.

APPENDIX II. NOTATION

The following symbols are used in this paper:

b = beam width;
E_x, E_y = moduli of elasticity in grain and across grain direction;
$f_{m,beam}$ = beam bending strength;
$f_{t,lam}$ = tensile strength of lamination;
G_c = fracture energy, critical energy release rate;
G_{xy} = shear modulus;
h = beam depth;
Δh = lamination thickness;
I = cross-sectional moment of inertia;
k_{lam} = laminating factor;
l = beam length;
M_c = critical bending moment;
α = beam depth ratio;
δ_n, δ_s = relative displacements across bondline;
ν = Poisson's ratio; and
φ = mixed mode angle at cracktip.